Rev. Roum. Sci. Techn.– Électrotechn. et Énerg.
Vol. xx, x, pp. 000–000, Bucarest, 20xx

RECONFIGURABLE INTELLIGENT SURFACE TUNED WITH NOMA FOR RESOURCE ALLOCATION

SAMPATH MADHUSUDHANAN[1], SAMUEL AMALORPAVA MARY RAJEE[2*], CHINNATHEVAR SUJATHA, MALU MANICKAM YAMUNA DEVI[4]

Keywords: Heterogeneous network; Non-orthogonal multiple access (NOMA); Reconfigurable intelligent surface (RIS); Resource allocation.

A reconfigurable intelligent surface (RIS) offers the potential benefits of 5G when combined with non-orthogonal multiple access (NOMA). As a result, the issues with distance, spectrum, and energy use worsen. Due to the limited energy supply, it is necessary to control the channel and achieve revolutionary energy efficiency that maximises both total rate and power optimisation. We jointly optimize the transmit power and optimal phase shift to mitigate the weak environment, thereby increasing the signal-to-noise ratio (SNR) and multiplexing data streams in the spatial domain. RIS arrays are used to form beams in the required directions. By decoupling the adjustable phase shift array elements, power allocation is performed using a low-complexity Dinkelbach method. The results are shown to provide practical solutions for users in different scenarios. The comparative results are shown to prove the novelty of the work and its significance.

1. INTRODUCTION

The widespread use of smartphones has led to a significant rise in both subscriber numbers and data traffic. Conversely, consumers find it challenging to fulfil their expectations for excellent service due to the wireless network's limited access to its resources. As a result, one of the potential approaches is to use an RIS-assisted NOMA system. It can be programmed as a smart device to manipulate incoming electromagnetic fields. The sizing of RIS elements varies from 100 square centimetres to 500 square metres.

By including sub-cells in the macrocell region, the system's spectral efficiency (SE) is enhanced compared to conventional mobile networks [1]. The number of reflecting elements in the arrays of the 5G base stations (BS) and user equipments (UE) can be measured at the order of 100 and 10, respectively. Macrocells are used in Hetnets to assure coverage, while small cells can be used in conjunction with macrocells to increase throughput [2]. Small base stations (SBSs) are easy to deploy and have good adaptability to deploy [3]. The employment of the BSs increases the power consumption of the wireless network. As a result, reducing interference, increasing energy efficiency, and increasing sum rate are what will determine how well RIS-assisted NOMA-based HetNet perform [4,5].

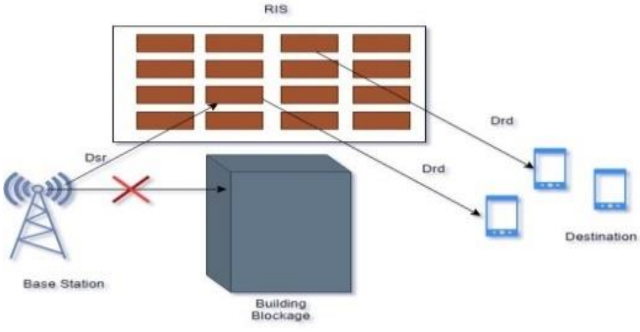

Fig.1 – RIS-enabled Heterogeneous network structure'

Figure 1 illustrates an RIS-enabled Hetnet structure where K users are associated with the BSs through both RIS links and direct links.

2. RELATED WORK

The authors in [6] suggested increasing the attainable rate of an RIS-enabled NOMA system, a simultaneous power allocation and reflection optimisation approach. Simulation findings show that, in comparison to traditional NOMA and RIS-assisted systems, the suggested algorithm can greatly increase system performance. The location and power allocation are jointly optimized, and the transmission beam forming is manipulated in an unmanned aerial vehicle [7]. The authors proposed a multiuser RIS-aided NOMA system with joint power allocation and channel estimation in [8]. The successive interference cancellation approach was employed to enhance the SE and EE NOMA. The signals are grouped according to their power. The NOMA convex function was used by the authors to suggest a game-theoretic technique for power control in HetNet. Fair resource distribution is also used among the consumers. Nearly one-third of the energy is used for operating the radio access network components. For several methods, including orthogonal frequency division multiple access, the authors in [8] addressed the radio resource allocation problems (OMA). Both schemes are deliberated as suitable techniques to support network metrics requirements for the users, and exploit multi-path fading to achieve high spectral efficiency.

The power domain is used by NOMA to achieve multiple access. It uses the successive interference cancellation (SIC) method specifically. With the help of this SIC technology, many users are multiplexed using various power levels within the same frequency range. The OMA scheme is very different from this. The NOMA system allows for the removal of interference from other users who have less channel state information (CSI) by the user who has more CSI. This is the reasoning behind NOMA's ability to use fewer spectrums than the OMA plan. [9-11]

The NOMA precept users should be superimposed at the same bandwidth, and interference results for such systems. As a result of the inclusion of additional interference that this new era brings, existing resource control mechanisms are utilized for ultra-dense networks. Although the NOMA strategy has several benefits, the increased statistics sensing

[1] Rajalakshmi Engineering College, Chennai, India.
[2] University of Witwatersrand, Johannesburg, South Africa (correspondence).
[3] Department of Computer Science and Engineering, SSM Institute of Engineering and Technology, Dindigul, India.
[4] Koneru Lakshmaiah Education Foundation, AP, India.
E-mails: madhusudhan.s@rajalakshmi.edu.in, maryrajee.samuel@wits.ac.za, sujathacse@ssmist.edu.in, yamunadevimm@klu.edu.in.

DOI: 10.59277/RRST-EE.2025.70.4.24

capacity of more customers as a result of this approach leads to better safety and privacy danger. Therefore, a series of security issues at the communication layers must be resolved to utilize this method in building a strong, environmentally friendly, and highly effective network. [12–14].

The interference alignment technique enhances the sum rate in a HetNet by mitigating interference among multiple users [15–17]. For MU-MIMO systems based on NOMA, user-centred techniques such as user-pairing and clustering are suggested.

To determine closed-form equations for sum-rate, outage probability, energy efficiency, and node power consumption under the NOMA uplink protocol, a mathematical approach is developed. These expressions in closed form can be used to create an optimisation issue that encapsulates the entire system. The difficulty of identifying the ideal parameters that maximise the amount of energy captured while maintaining reasonable system performance within the confines of communication is the impetus for this purpose.

The contributions are as follows:

- We derive expressions for the sum rate for the NOMA user of the proposed RIS-enabled NOMA HetNet.
- Initially, we jointly formulate the optimal phase shift and transmit power as a dual convex problem to calculate the SINR and then derive the closed-form expressions of the sum rate.
- Additionally, we demonstrate the impact of the power allocation ratio and adjustable phase shift on network performance.
- Finally, the proposed RIS-assisted NOMA HetNet is compared to its corresponding OMA counterpart and the case with RIS phase array elements.

3. SYSTEM MODEL

The capacities, coverage, transmit powers, and densities of base stations (BSs) that comprise a HetNet's n-tiered structure are what set them apart from one another. A two-tier heterogeneous uplink cellular network is modelled in this section. The macro base stations are accumulated with the tiny base stations in a two-tier HetNet. The idea behind Hetnet is to layer small cells over macro cells, providing functionality that the macro cell cannot handle on its own, while also meeting user traffic requirements and low-latency requirements. Within a circular radius of this RIS-enabled NOMA-based HetNet, one MBS and n number of SBS are situated.

A set of users, denoted as "$u_1, u_2, u_3, ..., U_n$", are connected to the BSs wherever the signal strength is possible. To prevent interference, users are divided into separate channels—the number of subchannels shares the entire system bandwidth. Users are assigned to specific subchannels according to their requirements. The users associated with SBS are denoted as SUE, and users associated with the macro base station are denoted as MUE. The adjustable phase shift coefficients of UEs and channel gain are assumed as $g = [g_{1,....,}g_M]^H \in \mathbb{C}^{M\times 1}$, and $h = [h_1, \dots \dots \dots h_M]^H \in \mathbb{C}^{M\times 1}$. The channel gain from the MUE to the RIS and from the RIS to the MBS is assumed as $[\Phi_1, \dots, \Phi_M]^H$.

The reflecting coefficients of the RIS is defined as $\Phi_M = \beta_m e^{j\theta_m}$, where β is an amplitude coefficient of value $\beta_m \in [0,1]$ and θ_m is the adjustable phase shift coefficient of value $\theta_m \in [0,2\pi]$.

The communication links blocked by the blockages are eradicated using RIS. The reflecting elements are adjusted with adjustable phase shift to provide connectivity [6,7]. The SINR of the UE is

$$\gamma^{UE} = \frac{P|g^H\Phi h + g^{SS}|^2}{Ph^S + \sigma^2} \quad (1)$$

Here σ^2 is the noise power at the receiver. In RIS-based NOMA systems, the outage probability is defined as the probability of the low SINR value, which is less than the threshold value γ_{th}

$$O_p = \Pr(\gamma < \gamma_{th}) \quad (2)$$

The objective function is to optimize the transmit power. It is represented as

$$P^* = \frac{Ph^{MM} - \gamma^{min}\sigma^2}{\gamma^{min}|g^{SM} + f^H\Phi h|^2} \quad (3)$$

The optimal transmitted power represented as P^* and the controllable phase shift of the M^{th} reflecting element is Φ_M. β, and x are the power allocation coefficient and data symbol selected from QAM constellations

The received signal is arranged in ascending order to refine the strongest signal in the cluster of uplinks and the weakest signal in the group. The sum rate of users of BS b on sub channel s is given by:

$$\sum_{i=1}^{4} \mathrm{R_i} \le \log_2\left(1 + \frac{\sum_{i=1}^{4} P_i}{N_0}\right) \quad (4)$$

where P_i stands for the i^{th} user's equivalent transmission power, and N_0 stands for the AWGN. It is assumed that there are four activated users in a multiple-access scenario (1, 2, 3, 4). The equivalent transmission powers of the four users are estimated to range from 4 dBm to 20 dBm.

Although the traditional direct superimposition scheme is capable of being the most useful perspective of information, the development and deciphering complication is extraordinarily excessive when the number of people is large. Therefore, a subchannel matching algorithm is proposed for uplink access.

As a result of RIS-enabled NOMA assigning various users to a subchannel through SIC, decoding is performed on the receiver, where interference is minimized in a positive order according to the power or channel advantage of different customers. The phase shift coefficient is optimized, and the rate maximization is denoted as

$$\begin{aligned} &\max \log_2(1 + \gamma^{UE}), \\ &s.t\ C_1: |\gamma^{UE}| \ge \gamma^{min}, \\ &C_2: |\Phi_m| = 1,\ \forall m, \\ &C_3: 0 \le P^* \le P^{max}. \end{aligned} \quad (5)$$

There is a maximum of users expected to be assigned to each subchannel of the BS. The users are first decoded at the identical subchannel. The data rate is in proportion to its SINR, and it can be formulated as follows, based on Dinkelbach's method,

$$\max R\ |g^H\Phi h + g^{SS}|^2 - \lambda|g^{SM} + f^H\Phi h|^2. \quad (6)$$

The achievable rate of the NOMA user is denoted as

$$\gamma_k^{NOMA} = \frac{P_k|g_k^{SS} + g_k^H\Phi h|^2}{|g_k^{SS} + g_k^H\Phi h|^2 \sum_{i=1}^{k-1} P_i + |h_k^{MS}|^2 P + \sigma_k^2}. \quad (7)$$

The interference lies in the first term of the denominator. The total sum rate is obtained as

$$R = \sum_{k=1}^{K} \log_2(1 + \gamma_k^{NOMA}). \quad (8)$$

3.1 TRANSMISSION POWER OPTIMIZATION WITH Φ

Resource allocation and subchannel allocation are done in an effort to cut down on system energy use. The successive convex approximation for low complexity

(SCALE) algorithm in [12],

For any $z > 0$,

$$\log_2(1+z) \geq \alpha \log_2 z + \beta \tag{9}$$

In eq. (6), the auxiliary variables are $\alpha = \frac{z_0}{1+z_0}$ and $\beta = \log_2(1+z_0)$, these are approximation constants.

The elements required for network QoS are maximum power constraints, CSI, and the rate of uplink users. The relationship is close-fitting when $z = z_0$. All these parameters have an adequate impact on the sum-rate maximization in RIS-NOMA, primarily based on HetNets. The optimisation problem is complicated by the following restrictions, such as the power need and the QoS requirement on each subchannel, to maximise the sum rate and minimise cross-tier interference. As a result, the following is the optimized sum rate

$$R = \sum_{i=1}^{K} \alpha_k \log_2 \gamma_k + \sum_{k=1}^{K} \beta_k \tag{10}$$

was denoted as the minimal required transmission rate of each BS.

$$max \sum_{k=1}^{K} \alpha_k \log_2\left(\left|g_k^{SS} + g_k^H \Phi h\right|^2 0\right) - \sum_{k=1}^{K} \beta_k -$$
$$- \sum_{k=1}^{K} \alpha_k \log_2\left(\sigma_k + \left|g_k^{SS} + g_k^H \Phi h\right|^2 \sum_{i=1}^{k-1} e^{P_i^*}\right)$$
$$s.t \ C_4: \sum_{k=1}^{K} e^{P_k} \leq P^{max}$$
$$C_5: \sum_{k=1}^{K} e^{P_k} |g_n^{SS} + f_n^H \Phi h|^2 \leq I_n^{th}, \forall n. \tag{11}$$

The optimization problem is a concave maximization, as the log-sum-exp function is convex [13]. The closed-form solution is obtained by solving the Lagrange dual theory. The solution can be solved as

$$L(P_k^*, \mu, \delta_n) = \sum_{k=1}^{K} \alpha_k P_k + \sum_{k=1}^{K} \alpha_k \log_2(\left|g_k^{SS} + g_k^H \Phi h\right|^2) - \sum_{k=1}^{K} \beta_k - \sum_{k=1}^{K} \alpha_k \log_2\left(\sigma_k + \left|g_k^{SS} + g_k^H \Phi h\right|^2 \sum_{i=1}^{K-1} e^{P_i}\right) + \mu(P^{max} - \sum_{k=1}^{K} e^{P_k}) + \sum_{n=1}^{N} \delta_n (I_n^{th} - \sum_{k=1}^{K} e^{P_k} |g_n^{SM} + f_n^H \Phi h|^2) \tag{12}$$

The non-negative multipliers are μ and δ. Based on Karush-Kuhn-Tucker (KKT) conditions, the transmitted power is calculated by

$$P_k^* = \left[\frac{\alpha_k}{\mu + \sum_{n=1}^{N} \delta_n |g_n^{SM} + f_n^H \Phi h|^2}\right]. \tag{13}$$

The main objective function is non-concave since $P_k^* \Phi_k$ and Φ_k are combined. Hence, we need to optimize the phase shift Φ_k in accordance with the solution (13) P_k^*.

3.2 ENERGY-EFFICIENT PHASE SHIFT OPTIMIZATION

The maximization of transmission power and phase shift of the RIS is optimized. To optimize Φ_k, the optimized transmit power should be fixed,

$$max \sum_{k=1}^{K} \frac{\alpha_k P_k \left|g_k^{SS} + g_k^H \Phi h\right|^2}{\left|g_k^{SS} + g_k^H \Phi h\right|^2 \sum_{i=1}^{k-1} P_i + \sigma_k},$$
$$s.t \ C_2: |\Phi_m| = 1 \ \forall \ m$$
$$C_6: \sum_{k=1}^{K} P_k |g_n^{SM} + f_n^H \Phi h|^2 \leq I_n^{th}. \tag{14}$$

A less complex and more effective set of multiple-ratio fractional programming is created to determine the non-convexity subjected to constraints C_2 and C_6. C_6 becomes

$$|g_n^{SM} + f_n^H \Phi h|^2 \leq |g_n^{SM}|^2 + |\Phi^H f|^2 = |g_n^{SM}|^2 + \Phi^H f \Phi \leq I_n^{th} \Big/ \sum_{k=1}^{K} P_k. \tag{15}$$

Thus, the phase shifts become

$$\Phi^H f \Phi \leq I_n^{th}, \tag{16}$$

where $I_n^{th} = I_n^{th} \Big/ \sum_{k=1}^{K} P_k - |g_n^{SM}|^2$ is the minimum interference for the macro UE,

$$max \sum_{k=1}^{K} y_k,$$
$$s.t. \ C_4: \Phi^H \cup \Phi = 1,$$
$$C_7: f_k^H + f_k \leq 0,$$
$$C_8: \Phi^H F \Phi \leq I_n^{th}, \forall \ n, \tag{17}$$

where $f_k = \Phi^H g_k g_k^H \Phi + 2\mathrm{Re}\{g_k^{SS} g_k^H \Phi\}$

The above problem is a convex optimization with quadratic constraints. Thus, the Lagrange function is

$$L(\Phi. y_k, \vartheta, \rho, \omega) = -\sum_{k=1}^{K} y_k + \vartheta(\Phi^H \cup \Phi - 1) + \sum_{k=1}^{K} \omega(f_k^H + f_k) + \sum_{n=1}^{N} \rho(\Phi^H F \Phi \leq I_n^{th}). \tag{18}$$

where ϑ, ρ and ω are the non-negative Lagrange multipliers.

Based on KKT conditions, the optimized phase shift becomes

$$y_k^* = \frac{\alpha_k P_k + \sigma\sqrt{\omega, \alpha, \rho}}{\sum_{i=1}^{K-1} P_i}. \tag{19}$$

The Lagrange multipliers are

$$\omega(l+1) = [\omega(l) + d_3(l) \times \{f_k^* + f_k\}], \tag{20}$$
$$\vartheta(l+1) = [\vartheta(l) + d_4(l) \times (\Phi^H \cup \Phi - 1)], \tag{21}$$
$$\rho(l+1) = [\rho(l) + d_5(l) \times (\Phi^H F \Phi - I_n^{th})], \tag{22}$$

where $d_3(l)$, $d_4(l)$ and $d_5(l)$ are the step sizes.

Uplink users on BSs and subchannels are assigned through the use of a matching technique. This collection of guidelines covers two main methods. The consumer is first assigned to the subchannel in accordance with the channel's exceptional status. If not, the relevant subchannel is allotted to the users with the highest CSI. Second, users who can increase the channel's EE are chosen.

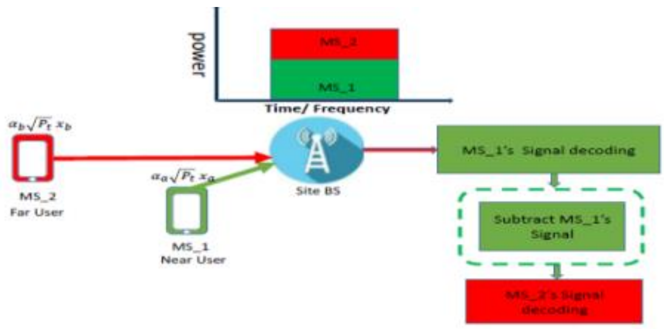

Fig. 2 – Uplink NOMA resource allocation.

Figure 2 is the uplink resource allocation plan for each BS. Because the exhaustive technique, the most effective resource allocation strategy, seeks all possible customer combinations and selects the consumer mixtures from them to maximise the power efficiency of the system, which significantly increases the complexity.

RIS NOMA-based Resource Allocation Algorithm

1 **Input:** **M,K,N,** $P^{max}, I_n^{th}, \sigma_k^2, g_k, h, f_n, g_n^{SM} g_k^{SS} h_n,$

2 **Initialize:** $\alpha_k, \beta_k, l = 0, P_k(0) = \frac{P^{max}}{K},$ $\delta(0) > 0,$

$$\vartheta(0) > 0,$$
$$\rho(0) > 0,$$
$$\omega(0) > 0,$$
$$d_3(0) > 0,$$
$$d_4(0) > 0, d_5(0) > 0$$
$$\Phi(0) = \frac{\pi}{2} I_M$$

3 While $l < L_{max}$ do
4 Update $P_k, \forall\, k$: (eqn)
5 **for** $i = 1{:}1{:}L_1$ do
Update Lagrange multipliers μ and δ by problems
Update auxiliary variable $\alpha_k(i+1) = \frac{\gamma_k^{UE}(i)}{1+\gamma_k^{UE}(i)}$
and $\beta_k(i+1) = \log_2\left(1+\gamma_k^{UE}(i)\right) - \alpha(i)log_2(\gamma_k^{UE}(i))$
6 **Check if** all the users are assigned with optimal power $\|P(i+1) - P(i)\|^2 < \varepsilon$ then
Obtain the next optimal $P^* = P(i+1)$
7 **end if**
8 **end for**
9 **Update** Φ for given P^*
for $j = 1{:}1{:}L_j$ do
Update the auxiliary variable y_k and the Lagrange multipliers
Until $\|y(j+1) - y(j)\|^2 < \varepsilon$
Obtain y_k, ω, α and ρ
If $\|\Phi(j+1) - \Phi(j)\|^2 < \varepsilon$ then
$\Phi^* = \Phi(j+1)$, break;
else
$j = j+1$;
end if
10 **end for**
Output P^* and $\boldsymbol{\Phi}^*$

The power and phase shift optimized performance parameters are initialized, along with the maximum iteration range and their error tolerance. Iteratively, the power matrix and subchannel allocation matrix are updated in accordance with the signal strength, and the total sum rate is determined. The sum rate restrictions are taken into consideration when updating the subchannel allocation matrix. The system's sum rate converges as a result of the increased repetition of iterations. The iterative strength optimisation set of rules' specific phases are enumerated in the algorithm.

$$\max \gamma,$$
$$s.t. \gamma \geq 0. \tag{23}$$

In terms of fundamental structure and functionality, RIS-based NOMA performs similarly to the sub-gradient approach. According to Dinkelbach's scheme, users with strong channel conditions perform the decoding; therefore, the messages of the weak user are decoded first by users with superior channel conditions. To help other users with weak channel states and increase their reliability, users with good channel conditions utilize this knowledge to act as relays for other users. Furthermore, the computational complexity of the proposed algorithm depends on the convergence precision parameter ε and the maximum iteration count L_{max}.

4. NUMERICAL EVALUATION AND SIMULATION RESULTS

This section presents analytical results from MATLAB simulations, where we consider a circular area 500 m in diameter, with the MBS located at its center. The FBS (K=4) and the number of reflecting elements (M) are varied from 4 to 200. The proposed resource allocation algorithm and power control in terms of rate are verified with the simulation. The simulation parameters are listed in Table 1.

Four users are supposed to be served by the small cell. Phase shift, power control, and resource allocation are derived simultaneously. We first derived the power control matrix, then the phase shift parameters. We successfully applied the suggested approach to enhance multiple performance measures simultaneously. For instance, when compared to the standard NOMA scheme, the system capacity and throughput gain increased by 19% and 26%, respectively, and by 81% and 66%, respectively, when compared to the conventional OFDMA scheme.

Table 1

Simulation parameters

Parameters	Values
Radius	500 m
System Bandwidth	1 MHz
Number of subchannel	10
Small cell radius	15 m
Transmission power of MBS	46 dBm
Transmission power of SBS	20 dBm
Noise power spectral density	-174 dBm/Hz

The suggested RIS-assisted NOMA implementation also enabled a significant increase in sum-rate. Similarly, the power allocation factor for the near user is β = 0.25, while for the far user it is β = 0.5.

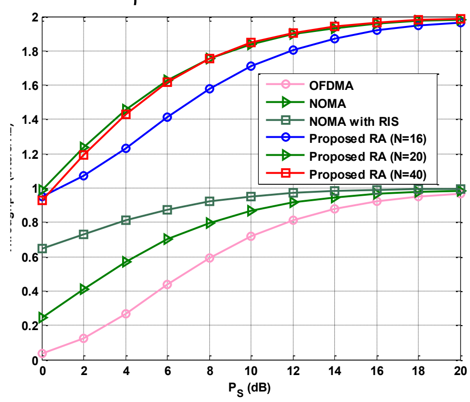

Fig. 3 – Throughput of NOMA-based HetNet over different reflecting elements.

We have assessed the scenario by adding more UEs. Based on the distance between users and the BSs, the effect of the power allocation factor is assessed on the performance of the RIS-NOMA system accordingly. The average throughput of the suggested resource allocation algorithm is shown in Fig. 3, and this configuration is simulated using random channel realizations. According to the data, the throughput gradually increases in the low transmit power zone, from 2 dB to 20 dB, and then converges once it enters the high power range.

Utilizing NOMA, the effectiveness of the suggested subchannel allocation and fair power allocation methods is assessed, and the results are contrasted with those of the NOMA and OMA techniques.

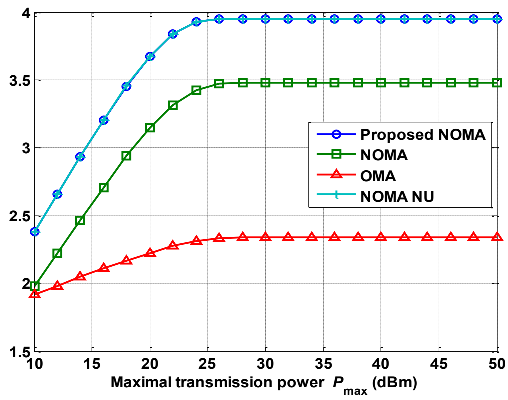

Fig. 4 – Average EE of NOMA-based HetNet over different Transmit powers.

Figure 4 illustrates how the energy efficiency performance of the proposed RIS-NOMA system is used to assess the impact of the power constraint.

It demonstrates that when the number of UEs increases, EE also rises, up to a point, that is, when the maximum system capacity is reached. However, if the number of UEs continues to rise, EE declines. But in HetNet, MBS fares better than SBS. However, throughput rises, but EE slightly drops as the number of UEs in the network rises. Additionally, this graph shows how RIS-assisted NOMA-based HetNets outperform other networks in terms of throughput and EE.

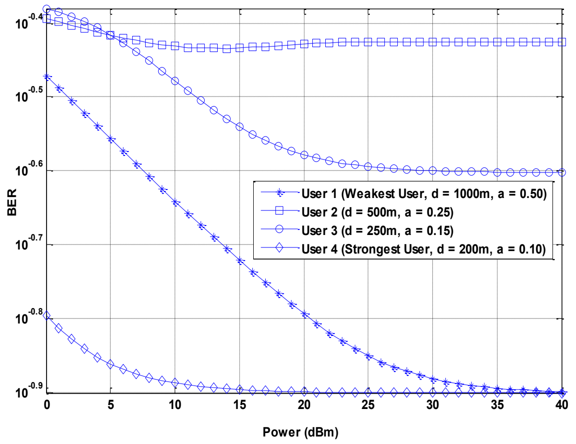

Fig. 5 – BER of RIS-NOMA-based HetNet over different transmit power.

The proposed NOMA system achieves a 6.1 dB increase in SNR for a BER of 10^{-2}. The ability of the proposed NOMA strategy to remove both the AWGN effect and cross-tier interference is what causes this increase in SNR. Figure 5 shows that the proposed RIS-NOMA scheme outperforms the SIC-based method [10] by approximately 24% in comparison. It should be noted that the RIS-based NOMA system requires additional processing and signalling overhead to carry out user pairing and power control operations, as well as to communicate this information to the ultra-dense network. According to the proposed results, the signal from the far end is considered interference. The likelihood of a failure, known as an outage, is the rate at which a message will be correctly decoded. The increase in target data rates for users depends on the outage probability. Hence, by using this subchannel allocation with power coefficients, we can mitigate an outage by adjusting channel coefficients and power coefficients.

The sum rate is varied in terms of the maximal transmit power in dBm. The linear increase is found from 10 dBm to 50 dBm. The proposed RIS-based NOMA outperforms well when compared with NOMA without RIS and OMA. Figure 6 depicts the improvements in sum rate.

Figure 7 depicts the energy consumption ratio during decoding and encoding steps. The higher the power factor coefficients, the higher the consumption. The maximum power consumption will have an impact on the energy performance.

This system can be applied for both smart and efficient data transmission under NOMA uplink. Near and far NOMA users are attempting to adjust their transmitted signals using their power factors. The power of RIS-NOMA is demonstrated in its application to planning and development in challenging environments.

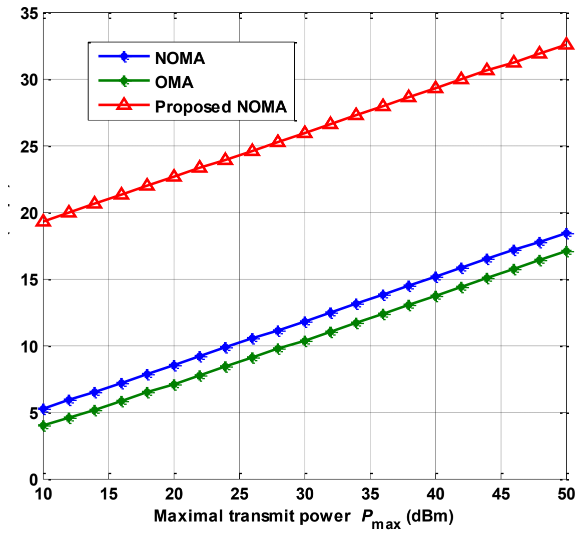

Fig. 6 – Sum-rate of RIS NOMA-based HetNet over Transmit power.

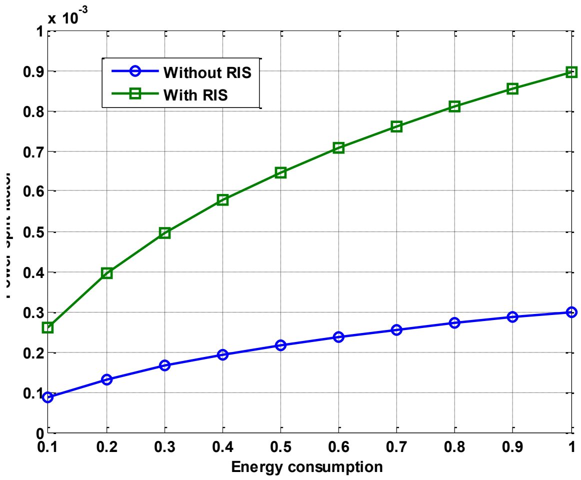

Fig. 7 – Energy consumption for users.

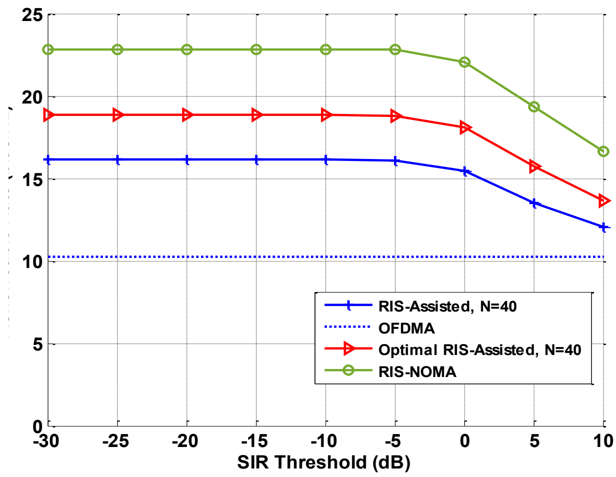

Fig. 8 – Achievable Rate of RIS-assisted NOMA users.

Analytical proof is demonstrated using the numerical data provided. Figure 8 is the depiction of the achievable data rate over the use of RIS-assisted NOMA. In three different array element scenarios, data rate and throughput in the presence of random phase shift and optimal phase shift are compared.

Table 2

Comparative analysis with other technologies.

Key parameters	Spectral Efficiency	Energy Efficiency	Hardware complexity	Coverage	Implementation cost	Computational complexity
Massive MIMO	Very high through spatial multiplexing and array gain	Moderate due to RF chain power consumption	High	Good	High due to RF chains.	Very High
Beamforming	High when focussing signal energy	Moderate , Requires phase shifters and power amplifiers	Moderate to High	Good	Moderate to High due to phase shifters	Moderate
Cognitive Radio	High through spectrum access	Moderate due to spectrum sensing	Moderate	Limited	Moderate due to hardware	Moderate
Cooperative communication	Moderate depending on relying technique	Low due to active relaying	Moderate to high	Good	Moderate due to multiple active nodes	Moderate to high
RIS-NOMA (Proposed)	Very high due to NOMA's multiplexing in power domain plus RIS channel conditions	Excellent due to passive elements with no power amplifiers for RIS	Low for RIS and moderate for NOMA	Excellent	Low to moderate due to passive RIS elements.	Moderate

5. CONCLUSION

In this work, the investigation of sub-channel allocation and energy optimization in RIS-NOMA-based HetNets with a focus on power limitations and cross-tier interference reduction is presented. Power optimisation through energy harvesting is suggested due to power limitations. Since the non-concave aim characteristic has a fractional shape, it can be transformed into an equivalent subtractive shape. The suggested and tested subgradient resource allocation algorithm is mostly dependent on the channel circumstances. The idea of phase shift optimization and power transfer occurring simultaneously is incorporated and examined, and the current trade-off between information rate and transferred energy at the receiver is illustrated. The proposed solution was able to adjust the phase shift and the user's transmission power, ultimately reaching the maximum data rate.

CREDIT AUTHORSHIP CONTRIBUTION

S. Madhu Sudhanan: presented idea, simulation
S. Amalorpava Mary Rajee: conceptualization
C. Sujatha: results analysis and data.
M.M. Yamuna Devi: designed

Received on 30 July 2024

REFERENCE

1. P. Swami, V. Bhatia, S. Vuppala, and T. Ratnarajah, *User Fairness in NOMA-HetNet Using Optimized Power Allocation and Time Slotting*, IEEE Systems Journal, **15**, *1*, pp. 1005–1014 (2021).
2. M. Marinescu and M. Morega, *Exposure of active medical implant bearers to electromagnetic emissions from wireless power transfer systems*, Rev. Roum. Sci. Techn. – Électrotechn. et Énerg., **67**, *2*, pp. 213–218 (2022).
3. H. Zeng, X. Zhu, Y. Jiang, Z. Wei, S. Sun, and X. Xiong, *Toward UL-DL Rate Balancing: Joint Resource Allocation and Hybrid-Mode Multiple Access for UAV-BS Assisted Communication Systems*, IEEE Trans. Commun., **70**, pp. 2757–2771 (2022).
4. M.R. Zamani, M. Eslami, M. Khorramizadeh, and Z. Ding, *Energy efficient power allocation for NOMA with imperfect CSI*, IEEE Trans. Veh. Technol., **68**, *1*, pp. 1009–1013 (2019).
5. Y. Su, X. Pang, W. Lu, N. Zhao, X. Wang, and A. Nallanathan, *Joint Location and Beamforming Optimization for STAR-RIS Aided NOMA-UAV Networks*, IEEE Transactions on Vehicular Technology (2023).
6. O. Maraqa, A.S. Rajasekaran, S. Al-Ahmadi, H. Yanikomeroglu, and S.M. Sait, *A survey of rate-optimal power domain NOMA with enabling technologies of future wireless networks*, IEEE Communications Surveys & Tutorials, **22**, *4*, pp. 2192–2235 (2020).
7. J. Seo and Y. Sung, *Beam design and user scheduling for non-orthogonal multiple access with multiple antennas based on Pareto optimality*, IEEE Transactions on Signal Processing, **66**, *11*, pp. 2876–2891 (2018).
8. Q.-U.-A. Nadeem, A. Kammoun, A. Chaaban, M. Debbah, and M.-S. Alouini, *Intelligent reflecting surface-assisted multi-user MISO communication* (2019).
9. C. Chih-Lin, C. Rowell, S. Han, Z. Xu, G. Li, and Z. Pan, *Toward green and soft: a 5G perspective*, IEEE Communications Magazine, **52**, *2*, pp. 66–73 (2014).
10. A. Agçal, A. Kalay, and R. Cetin, *Wireless power transfer for underwater vehicles*, Rev. Roum. Sci. Techn. – Électrotechn. Et Énerg., **68**, *2*, pp. 194–199 (2023).
11. X. Cheng, Y. Hu, and L. Varga, *5G network deployment and the associated energy consumption in the U.K.: A complex systems' exploration*, Technol. Forecasting Social Change, **180** (2022).
12. D. Zhang, Q. Wu, M. Cui, G. Zhang, and D. Niyato, *Throughput maximization for IRS-assisted wireless powered hybrid NOMA and TDMA*, IEEE Wireless Commun. Lett., **10**, *9*, pp. 1944–1948 (2021).
13. A.M. Rajee, A. Merlin, and M.M. Yamuna Devi, *Game Theoretic approach for power control in next generation Heterogeneous Networks*, Signal, Image and Video Processing (2023).
14. D. Zhang, Q. Wu, M. Cui, G. Zhang, and D. Niyato, *Throughput maximization for IRS-assisted wireless powered hybrid NOMA and TDMA*, IEEE Wireless Commun. Lett., **10**, *9*, pp. 1944–1948 (2021).
15. S.A.M. Rajee and A. Merline, *Machine intelligence technique for blockage effects in next-generation heterogeneous networks*, Radioengineering, **29**, *3* (2020).
16. W.U. Khan, X. Li, A. Ihsan, Z. Ali, B.M. Elhalawany, and G.A.S. Sidhu, *Energy efficiency maximization for beyond 5G NOMA-enabled heterogeneous networks*, Peer-to-Peer Netw. Appl., **14**, pp. 3250–3264 (2021).
17. A.K. Varma, B. Kumar, A. Ramakrishna, and D. Mitra, *Multi-hop relay selection for cooperative sensing in cognitive radio networks*, Rev. Roum. Sci. Techn. – Électrotechn. Et Énerg., **69**, *2*, pp. 237–242 (2024).